BEAM PROPERTY MEASUREMENTS ON THE KU-FEL LINAC

K. Masuda*, K. Hayakawa, T. Kii, S. Murakami, H. Ohgaki, T. Yamazaki, K. Yoshikawa, H. Zen,
Inst. of Advanced Energy, Kyoto Univ., Gokasho, Uji, Kyoto 611-0011, Japan

Abstract

An infrared FEL facility, KU-FEL, is under construction for advanced energy researches. An S-band rf gun and an accelerating tube has been installed. Measurements of beam properties have been carried out. An energy spread below 1 % at 50 mA current has been obtained. The normalized emittances were measured to be 78 π mm mrad in horizontal and 70 π mm mrad in vertical directions by the tomographic technique. A dipole sweep magnet was set for sweeping the back-streaming electrons vertically out of the cathode in the rf gun. It is found that the magnet does not affect the beam emittance, but results in poor current transmittance through the linac. PARMELA simulation suggests the use of a horizontal Sweep magnet instead of the vertical one.

INTRODUCTION

An infrared FEL facility, KU-FEL[1,2], is under construction for researches on advanced sustainable energies, such as bio-energy, solar energy. An electron beam of 30 MeV has been obtained by an S-band rf gun with a thermionic cathode and a recently installed accelerating tube. In this paper, we will describe measurements of the beam properties on the KU-FEL linac, such as transverse emittance, energy spread, and beam current. Comparison with PARMELA[3] simulations will be also presented.

One of the critical R&D issues on our KU-FEL linac is that of reducing and/or compensating the adverse effect due to back-streaming electrons onto the cathode, and time-varying beam-loading and accordingly time-varying output beam energy during a macropulse [4], inherent in thermionic rf guns. The introduction of transverse dipole magnetic fields along the cathode surface [5] has been found effective against this back-bombardment effect in our rf gun [6], while effects of the induced transverse beam deflection on the output beam transport through the linac as well as the beam emittance have not been evaluated. In this paper, we will discuss comparisons of the beam properties with and without the transverse B-field in the vicinity of the cathode.

EXPERIMENTAL SETUP

The KU-FEL linac consists of an S-band 4.5-cell rf gun with a thermionic cathode, a 3-m accelerating tube, and a beam transport system, shown schematically in Fig. 1. The typical output energy by the gun is 9 MeV. An energy analyzer consisting of a 45-degree bending magnet and a horizontal slit is located between the gun and the accelerating tube. The energy analyzer is followed by 3 quadrupole magnets and another dipole which comprise an achromatic transport system (Dog-Leg section in Fig. 1) to the accelerating tube. The designed maximum beam energy is 40 MeV, which will be led through the 180-degree arc section into the undulator to be installed to produce 4-13 μm IR-FEL [7].

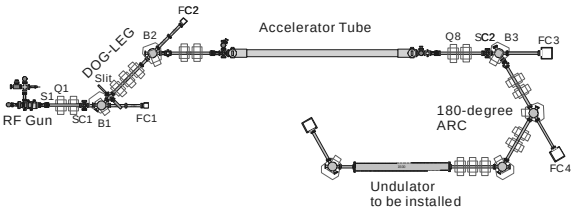

Figure 1: Schematic view of the KU-FEL linac.

On one hand a thermionic rf gun has advantageous features over a photocathode one, such as low cost, easy operation, and high average current. On the other hand it inherently has some disadvantages such as current and energy fluctuations during a macropulse due to beam-loading and back-streaming electrons hitting the cathode. To cope with the last problem, we have set a dipole magnet (called 'Sweep magnet' hereafter) to sweep out the back-streaming electrons by providing horizontal transverse B-field along the cathode surface [5]. In order to compensate the resultant vertical beam deflection with respect to the gun axis, a steering dipole magnet set at the gun exit (S1 in Fig. 1) was used.

Also, aiming at a further reduction of back-streaming electrons, use of a cathode with smaller diameter in combination with the Sweep magnet is being studied [8]. In the present measurements, a tungsten dispenser cathode of 2 mm diameter was used instead of the cathode of 6 mm diameter previously used [9]. The cathode surface temperature was measured by an IR pyrometer and was fixed to 1473 K. The corresponding current density on the cathode surface is 38.1 A/cm^2.

Throughout the measurements, the macropulse duration of rf input to the gun was fixed to 2 μsec in order to minimize the degradation in the projected beam's properties owing to the time-variation during the macropulse. The rf input powers to the gun and the accelerating tube were 7 and 10 MW respectively. In this paper, the magnetic flux density by the Sweep magnet in the vicinity of the cathode was fixed to 29 gauss.

RESULTS AND DISCUSSIONS

Beam properties at the gun exit

Measurements of beam currents, transverse emittances, and energy spectra at the gun exit were carried out with

* E-mail: masuda@iae.kyoto-u.ac.jp

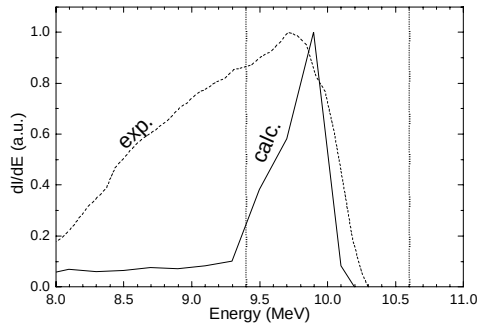

Figure 2: Energy spectra at the gun exit by the measurement (dashed line) and by the simulation (solid line). The dotted lines indicate the energy acceptance of the following energy slit (B1 and Slit in Fig. 1).

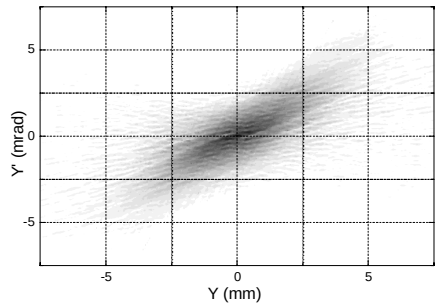

(a)

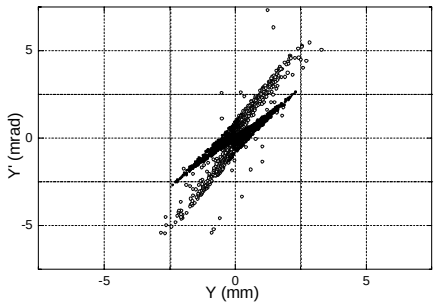

(b)

Figure 3: Vertical phase space distribution in the vertical direction, (a) reconstructed by the tomographic technique from the observed images in SC1 in Fig. 1, and (b) by the simuration. The black circles in (b) show particles within the major high energy component indicated in Fig. 2.

and without the Sweep magnetic field. The tomographic method described in [9] was applied for the measurements of the transverse phase space distributions and corresponding emittances, with a quadrupole magnet (Q1 in Fig. 1) and a phosphor screen (SC1). The energy spectra were taken with a bending magnet (B1) and a Faraday cup (FC2). The energy resolution was found to be $\Delta E/E$ = 13 % by a PARMELA run.

Introducing the Sweep magnet, the beam current, measured with a Faraday cup (FC1 in Fig. 1), was seen to decrease from 460 mA to 400 mA. No degradation in the transverse emittances in both horizontal and vertical directions was observed, while a slight improvement in the energy spread was seen, as stated in [8]. The experimental results in the case without the Sweep magnet are shown in Figs. 2 and 3, together with PARMELA results for comparisons.

Table 1: Unnormalized emittances at Q1 downstream the gun exit (see Fig. 1). The emittances by the simulation take only the high energy component indicated in Fig. 2 into account, while those in the parentheses include all particles. [π mm mrad]

		measurement	simulation
with Sweep magnet	horizontal	1.9	0.23 (0.18)
	vertical	1.8	0.23 (1.25)
w/o Sweep magnet	horizontal	1.8	0.21 (0.22)
	vertical	2.0	0.14 (0.23)

The energy spectra are shown in Fig. 2. The difference between the measured and the calculated energy spreads in the figure, may be due the time-dependent beam-loading effects during the macropulse which are ignored in the simulation. In the measurements downstream the Dog-Leg section, the energy acceptance of the energy slit was fixed to 10.0 ± 0.6 MeV, which is indicated in Fig. 2 by the dotted lines.

Figures 3 (a) and (b) show the phase space images in the vertical direction, and the corresponding emittances. Both the beam emittances with and without the Sweep magnet are listed in Table 1. The rotational angle in the phase space shown in fig.3, is reproduced well by the simulation, although appreciable differences in the corresponding emittances can be observed. As before this difference can be due to time dependent effects along the macropulse, and also to the broad energy spread in the reconstruction process in the tomographic measurement, which are neglected in the simulation, though extremely low energy component must be swept out of the phosphor screen (SC1) in the measurement also.

Beam properties at the accelerating tube exit

The beam without the Sweep magnetic field applied in the vicinity of the gun cathode was transported through the Dog-Leg section to the accelerating tube. The beam properties were measured at the accelerating tube exit, with a quadrupole magnet (Q8 in Fig. 1) and a screen monitor (SC2) for transverse emittances, and with a bending magnet (B2) and a Faraday cup (FC4) for the energy spectra.

For the SC2, either a 1-mm thick phosphor (chromium-doped alumina) or an aluminium plate can be used at exactly the same position. As it is seen in Fig. 4, the fluorescence profile from the phosphor screen is found broader than the transition radiation profile from the aluminium plate. The broadening was around 35 % in both horizontal and vertical directions, depending neither

Table 2: Beam currents [mA], from the gun down to the accelerating tube exit.

		gun exit	accelerating tube entrance	accelerating tube exit
experiments	w/o Sweep magnet	460	60	48
	with Sweep magnet	400	46	<5*
simulation	w/o Sweep magnet	633	197	65
	with Sweep magnet	520	105	20

*average over macropulse duration

on the incident beam angle of 0 and 45 degrees nor on the beam size of 2.2 and 1.6 mm in FWHM. Although this broadening with phosphor screen would result in an overestimate in the emittances, we used the phosphor screen, characterized by a much higher signal to noise ratio.

Reconstructed images by the tomographic technique in the transverse phase spaces are shown in Figs. 5(a) and (b). The resultant geometric emittances were 1.3 π mm mrad in horizontal and 1.2 π mm mrad in vertical, corresponding to normalized emittances of 78 and 70 π mm mrad.

Then we tried to transport the beam with the Sweep magnetic field applied, by changing the strength of the quadrupole magnets and of the steering magnet at the gun exit (S1 in Fig. 1). In contrast with the case without the Sweep magnet, the beam could hardly be transported through the accelerating tube, although, as presented in the previous section, almost no degradation in the beam properties were seen at the gun exit either in the measurement or the PARMELA simulation. So far, we have obtained beam currents listed in Table 2 from the gun exit to the accelerating tube exit. The tendency of a poor transmittance in the case with the Sweep magnet can be also seen in PARMELA results as summarized in the table.

Figure 6 shows the measured energy spectra with and without the Sweep magnet, both normalized as their peaks are unity. Although the energy resolution and signal to noise ratio were poor for the case without the Sweep magnet, the energy spread with the Sweep magnet was found 1.5 % (FWHM), and was found to be broader than the one obtained without the Sweep magnet (less than 0.7%). We can see this tendency more clearly in the PARMELA results in Fig. 7, showing that the energy spreads (FWHM) with and without the Sweep magnet were 2.4% and 0.49% respectively, which seem to agree with the experimental ones. From the simulations in Fig. 7 we can see that the sharp peak in the energy spectrum without the Sweep magnet was almost lost with respect to the case with the Sweep magnet.

As shown in the evolution of the beam envelope by the PARMELA simulations in Figs. 8 (a) and (b), we could hardly compensate the effects due to the vertical deflection induced by the Sweep magnet in the gun, even with an additional steering magnet between the gun and

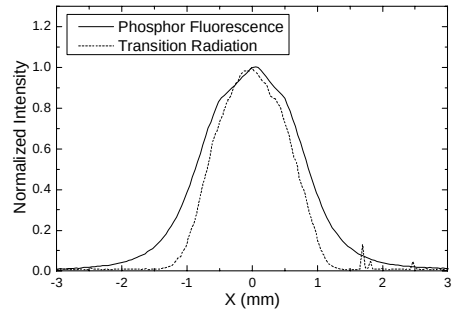

Figure 4: Comparison between the horizontal profiles of the fluorescence from the phosphor plate, and the transition radiation from the aluminium plate.

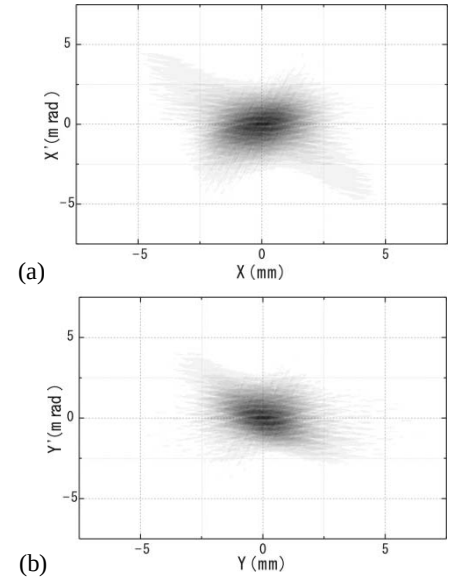

Figure 5: Transverse phase space distributions at the accelerating tube exit obtained with Q8 and SC2 in Fig. 1 in (a) horizontal and (b) vertical directions.

the following quadupole magnet (Q1). Then we performed PARMELA runs with a horizontal Sweep magnet instead of the vertical Sweep. In this case, because horizontal dispersion can be controlled in the quadrupole magnets in the Dog-Leg section, we could

find a set of the magnet parameters showing a better transmittace to the end as shown in Fig. 9. As a result, the calculated current at the accelerating tube exit was 181 mA.

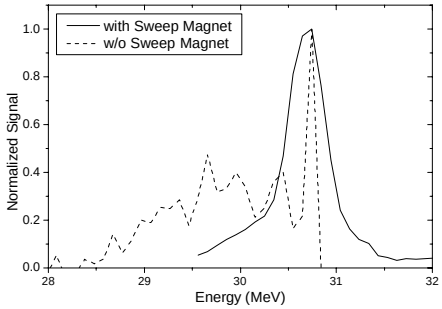

Figure 6: Measured energy spectra with and without the Sweep magnet, both of which are normalized to their peaks.

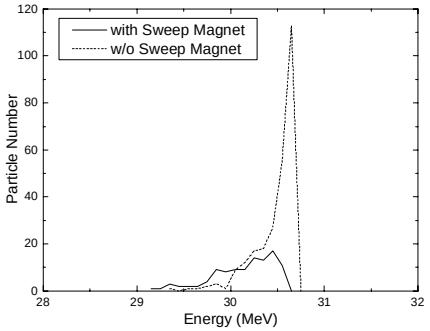

Figure 7: Energy spectra by the simulations with and without the Sweep magnet.

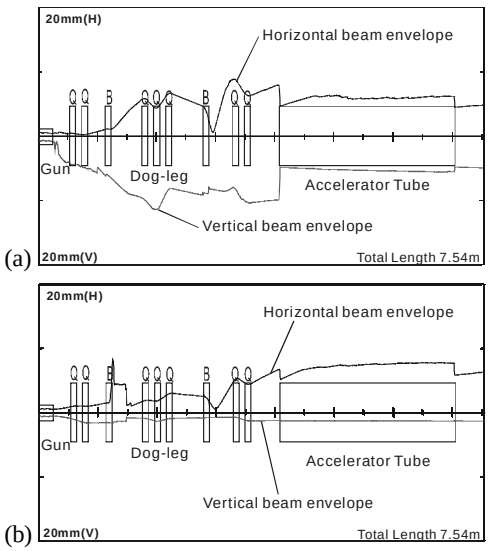

Figure 8: Calculated evolution of the horizontal and vertical beam envelopes, for the case (a) with and (b) without the Sweep magnet.

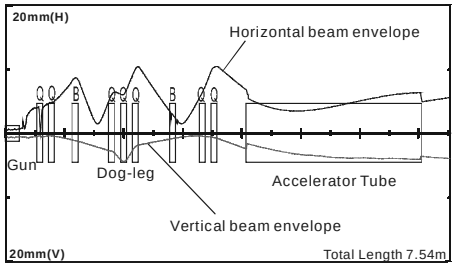

Figure 9: Calculated evolution of the horizontal and vertical beam envelopes with a horizontal Sweep magnet instead of the vertical one.

CONCLUSION

We have measured the electron beam properties, namely energy spread, and transverse emittances at the rf gun exit, and at the exit of the accelerating tube where the energy was measured to be 30.7 MeV. A beam with energy spread of less than 1 % and 48 mA current was obtained. The normalized emittances were measured to be 78 π mm mrad in horizontal and 70 π mm mrad in vertical directions by the tomographic technique with a phosphor screen.

A dipole (Sweep) magnet was set for sweeping the back-streaming electrons vertically out of the cathode in the rf gun. The induced beam deflection in the vicinity of the cathode was found not to degrade the output beam emittances in the present case. However, the vertical deflection by the Sweep magnet resulted in poor transmittance down to the accelerating tube exit. The simulation predicts that much better transmittance can be achieved by use of a horizontal Sweep magnet instead of the vertical one in our layout.

REFERENCES

[1] T. Yamazaki, et al., Proc. of 23rd Int'l FEL Conf. (2002) II13.
[2] T. Kii, et al., "Renewal of KU-FEL facility" in these proceedings.
[3] L. M. Young, J. H. Billen, PARMELA, LA-UR-96-1835.2001.
[4] K. Masuda, et al., Nucl. Instr. and Meth. A 483 (2002) 315.
[5] C.B. McKee and J.M. Maday, *Nucl. Instr. Meth.* A 296 (1990) 716.
[6] T. Kii, et al., Nucl. Instr. And Meth. A 507 (2003) 340.
[7] H. Ohgaki, et al., Nucl. Instr. And Meth. A 507 (2003) 150.
[8] T. Kii, et al., "Reducing back-bomdardment effect using thermionic cathode in IAE rf gun" in these proceedings.
[9] H. Ohgaki, et al., Nucl. Instr. and Meth. A 528 (2004) 366.